Geomechanics and Engineering, *Vol. 14, No. 2 (2018) 107-113*
DOI: https://doi.org/10.12989/gae.2018.14.2.107

Cracks evolution and multifractal of acoustic emission energy during coal loading

Xiangguo Kong[*1,2,3], Enyuan Wang[**1,2,3], Xueqiu He[3,4], Xiaofei Liu[1,2,3], Dexing Li[1,2,3] and Quanlin Liu[1,2,3]

[1]*Key Laboratory of Gas and Fire Control for Coal Mines, China University of Mining and Technology, Xu Zhou, Jiangsu 221116, China*
[2]*State Key Laboratory of Coal Resources and Safe Mining, China University of Mining and Technology, Xu Zhou, Jiangsu 221116, China*
[3]*School of Safety Engineering, China University of Mining and Technology, Xu Zhou, Jiangsu 221116, China*
[4]*College of Civil and Resource Engineering, University of Science and Technology Beijing, Beijing 100083, China*

(Received March 7, 2017, Revised June 9, 2017, Accepted June 27, 2017)

Abstract. Coal samples with different joints morphology were subjected to uniaxial compression experiments, cracks evolution was recorded by Nikon D5300 and acoustic emission (AE) energy signals were collected by AEwin Test for Express-8.0. During loading process, coal samples deformed elastically with no obvious cracks changes, then they expanded gradually along the trace of the original cracks, accompanied by the formation of secondary cracks, and eventually produced a large-scale fracture. It was more interesting that the failure mode of samples were all shear shape, whatever the original cracks morphology was. With cracks and damage evolution, AE energy radiated regularly. At the early loading stage, micro damage and small scale fracture events only induced a few AE events with less energy, while large scale fracture leaded to a number of AE events with more energy at the later stage. Based on the multifractal theory, the multifractal spectrum could explain AE energy signals frequency responses and the causes of AE events with load. Multifractal spectrum width ($\Delta\alpha$), could reflect the differences between the large and small AE energy signals. And another parameter (Δf) could reflect the relationship between the frequency of the least and greatest signals in the AE energy time series. This research is helpful for us to understand cracks evolution and AE energy signals causes.

Keywords: cracks evolution; multifractal; acoustic emission; load; coal

1. Introduction

With coal mining entering deep stage, stress increases with depth rapidly, which can induce rock outburst (Feng *et al.* 2016, Song *et al.* 2017, Yin *et al.* 2016, Yan *et al.* 2015). This disaster is how to be formed and developed, and how to monitor the mining disasters effectively, which have been hot problems in rock engineering and coal mining fields. Because AE is radiated during coal fracture and failure process (Al-Jumaili *et al.* 2015, Zitto *et al.* 2015, Liang *et al.* 2017), it's used to research coal or rock damage widely.

About AE signals research of coal or rock loading, there are many useful referenced studies (Li *et al.* 2016a, Kong *et al.* 2015, 2017). Shkuratnik *et al.* (2004, 2005) systematically studied AE characteristics of coal under different loading experiments. He *et al.* (2014) studied AE behaviors of coal specimen under triaxial cyclic loading and unloading conditions, and noted that the changes in AE energy coincided with the stress experienced by coal specimens. Ganne *et al.* (2007) considered that AE could reflect the degree of internal damage in coal and rock, which was directly related to the internal defect and damage evolution. Zou *et al.* (2014) found the pore structure of coal would change after gas drainage. Therefore, Majewska *et al.* (2006, 2007) discussed the chaotic behavior of AE induced in hard coal by gas adsorption–desorption. Kong *et al.* (2015, 2017) researched the critical slowing down characteristics of AE about coal containing gas, and concluded that the index of critical slowing down, such as variances and autocorrelation coefficients could play the precursory of coal failure. In order to built the relationship between AE parameters and coal burst disaster, Cao *et al.* (2007) researched AE characteristics in coal outbursts, and considered that this method could be used to predict dynamic disasters in coal mines. To reveal the regularities between AE signals and coal failure forward, the fractal characteristics of AE attracted many researchers. Gao *et al.* (2013, 2014) studied AE fractal regularities of coal under uniaxial and triaxial compression, and concluded that AE fractal characteristics behaved differently under different confining pressure. Kong *et al.* (2016) researched the fractal phenomenon of AE about coal containing gas which was loaded by triaxial compression. Li *et al.* (2009) found that the fractal dimension of AE and b values were similar in loading process.

AE can only reflect coal damage indirectly. If we want to watch cracks evolution process visibly, we need to capture cracks by digital video (Landis *et al.* 2003, Elaqraa *et al.* 2007, John *et al.* 2001). By digital image, Chen *et al.* (2014) analyzed damage evolution of rock with different angle cleats under uniaxial compression, and the results

∗Corresponding author, Ph.D.
E-mail: kxgtudou7218@163.com
∗∗Corresponding author, Professor
E-mail: weytop@263.net

ISSN: 2005-307X (Print), 2092-6219 (Online)

showed that the anisotropic damage evolution of jointed specimens was efficiently captured with the method of image analysis. The CT image was analyzed by the method of digital image processing, which included threshold partition, and then the real cracks morphologic was got (Tian *et al.* 2012). According to the CT images of the concrete samples obtained for each loading step, the cracks evolution images of the concrete samples were obtained using the digital image processing technology (Fang *et al.* 2015). Chen *et al.* (2013) studied the fractal characteristics of surface cracks evolution by the simulation of coal and gas outburst. Li *et al.* (2014) analyzed fractal characteristics of cracks and fragments generated in unloading rock burst tests. Based on microseismic monitoring technology, Liu *et al.* (2016) researched the fractal behaviors for the mining cracks evolution process of overlying strata.

Overall, about AE responses of loaded coal and rock, and cracks evolution images, there are a great number of achievements, which lay a foundation for the study of mechanical behavior of coal and rock (Wang *et al.* 2015, Li *et al.* 2016b). However, there are lack of studies about coal cracks evolution from direct and indirect aspects simultaneously. And cracks evolution with time is how to correspond with it along with load? What's the cause of AE signals during loading process? In this paper, cracks evolution with time of coal samples under axial compression were researched, and its changes with load were analyzed. What's more, the failure mode was explored forward. AE energy and the accumulated AE energy laws during loading process could reflect cracks evolution and damage changes of coal. The multifractal characteristics of AE energy signals revealed AE causes during loading process and built the relationship between AE and cracks evolution.

2. Experimental analysis

2.1 Experimental system

The experimental system consisted of an axial loading subsystem (Fig. 1(a)), an AE monitoring subsystem (Fig. 1(b)), and a digital video camera (Fig. 1(c)). The axial load and control subsystem was an electrohydraulic servo pressure-testing machine controlled by a microcomputer (YAW4306). The AE monitoring subsystem used was an AE data-acquisition system (AEwin Test for Express-8.0). A digital video camera (Nikon D5300) was used to capture the cracks evolution of coal samples during loading process. In all experiments, the loading rate was 20 N/s, the sampling frequency was set as 500 kHz and the threshold value was set as 45 dB.

2.2 Coal samples

The coal samples (50×50×100 mm size) were made from coal bulk, which was collected from DaAnshan coal mine, Beijing. According to ISRM, we prepared the coal samples to meet the requirements (the nonparallelism of two ends about samples need to be less than 0.05 mm). Among the various samples prepared, we chose 18 samples for the experiments. These coal samples had many primary cracks, and their joints were developed.

2.3 Experimental procedures

In these experiments, after preparing coal samples, the AE sensors were linked to the amplifiers and monitors firstly. Then the AE sensors were pasted on the designed positions of the sample surface with the help of coupling agent (Vaseline). Next, the prepared specimen was put on the test bench of loading subsystem, which was risen slowly until the top of coal sample contacted the top boundary of loading subsystem. Finally, the loading subsystem was started again, and the AE monitoring subsystem and the digital video camera were operated simultaneously until specimen failure. Repeat the test of the next sample according to the steps mentioned above. The experimental procedures can be summarized as follows (Fig. 2).

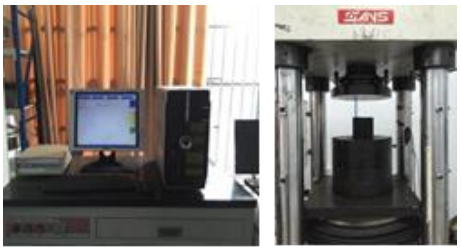

(a) Uniaxial loading subsystem

(b) AE monitoring subsystem

(c) Digital video camera

Fig. 1 Experimental system

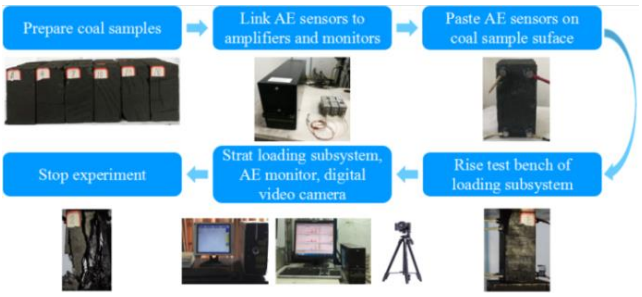

Fig. 2 Experimental procedures

3. Loading process of coal samples

3.1 Crack evolution

Coal sample 10 was chosen to analyze the cracks evolution, which could be seen in Fig. 3. From Fig. 3, we could obtain that sample 10 was of a few small cracks near the top end of it. From 0 s to 100 s, the number and shape of cracks didn't change, which indicated that the coal sample deformed elastically and was in capacity-bearing state. At 340 s, the cracks expanded gradually along the trace of the original cracks. Then the width of these cracks enlarged forward (350 s and 365 s), accompanied by the formation of secondary cracks. Most of these cracks joined together and produced a macroscopic fracture (400 s), which eventually leaded to the failure of the specimen. From time aspect, cracks initiation and expanding experienced for long time, while the failure occurred only a few seconds. This demonstrated that the energy accumulation needed long time and energy release was momentary. For example, when coal mined underground, the energy was accumulated in surrounding rock, which was a long process. However, the surrounding rock couldn't bear increasing stress, coal or rock burst would occur to release energy in a short period.

In order to illustrate the cracks evolution during the loading process, the cracks distribution of sample 10 with the load was analyzed in Fig. 4. When the load reached a peak load of 26.8%, there were no obvious changes of the macroscopic cracks on the sample surface. When the load reached 85.4% peak load, the upper right corner of the sample had a macroscopic crack, which gradually widened with the loading. And when the load reached the 87.8% peak load, a number of macroscopic cracks appeared on the surface of sample. However, when the coal sample was loaded to the peak load of 91.5%, the sample had been destroyed locally, with two pieces of coal bulk, close to the sample bottom, separating from the original sample. Because the sample still had bearing capacity, the load was still increasing along with further cracks evolution. When the load exceeded the peak load, the load-time curve showed a decline suddenly. It showed that coal was similar to rock in brittle property, which was also the reason that coal burst would happen in the mining process. When it was loaded to 400 s, that was, in the decrease process of load-time curve, lots of macro cracks formed on the sample surface with coal pieces separated from itself. There were similar phenomena in other experiments, due to length limitations, it's not described in this article.

3.2 Failure mode

In order to explore failure mode of coal samples under uniaxial compression, the coal samples 2, 5, 7, 8, 10, 11, 13 and 16 were selected to analyze it, which were shown in Fig. 5. And these coal samples had different original cracks shape. Joints or primary cracks would affect the mechanical properties of coal. At the bottom of sample 5, it was severely damaged because this sample had a larger bedding at the bottom. Therefore, it destroyed in crushing failure. The failure mode of samples 2, 8, 10, 11 and 13 was obvious shear failure. The sample 16 had several macroscopic vertical cracks formed, which seemed to be

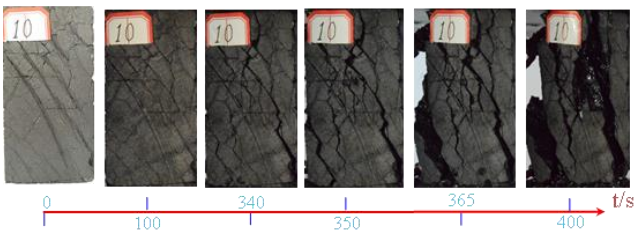

Fig. 3 Cracks evolution of coal sample 10

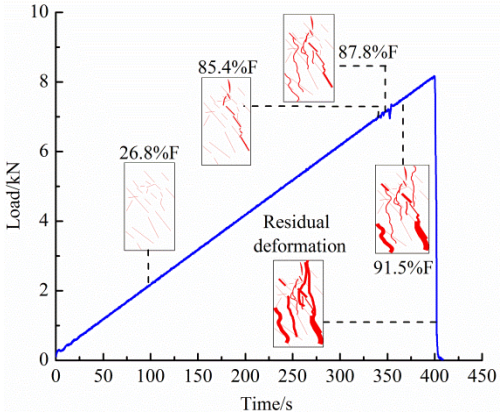

Fig. 4 Cracks evolution response with load

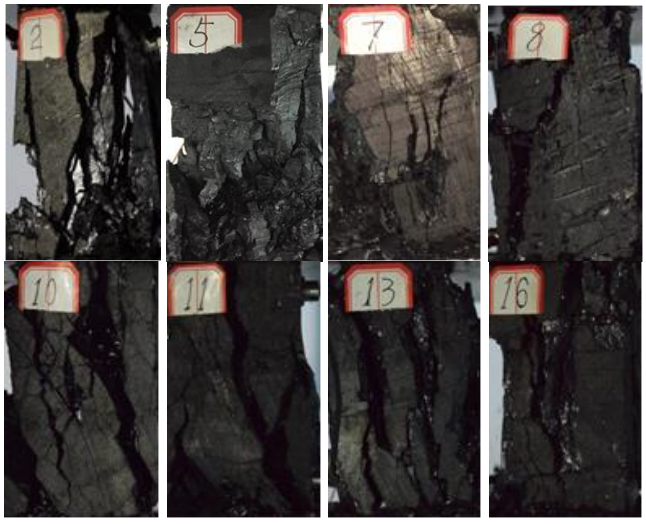

Fig. 5 Failure modes of coal samples

splitting failure under compression. In fact, the shear cracks were formed initially and vertical cracks were formed at failure time, so the shear stress dominated during loading process. In a word, the final failure modes of specimens were all shear failure, whether they were with the oblique joints, the cross cracks or without obvious joints.

4. Acoustic emission evolution and multifractal characteristics

4.1 AE energy evolution

During coal loading process, deformation energy is accumulated and released during various loading stages. In

this process, acoustic emission (Gao *et al.* 2014, Kong *et al.* 2015), electromagnetic radiation (Wang *et al.* 2011) and heat radiation produce with cracks evolution, so these energy variation can reflect damage evolution. AE energy data were collected to analyze cracks and damage changes. Fig. 6 showed AE energy, accumulated AE energy and load changed with time. From Fig. 6, we could conclude that AE response curves of the loading process were almost similar, regardless of whether they were with the oblique joints, the cross cracks or without obvious joints. At the initial loading stage and the elastic deformation stage, AE energy value was less. However, AE energy suddenly started to increase when load curve approached the peak load. Near the maximum load, AE energy reached the maximum. Once the coal sample couldn't bear increased load, it would be crushed, which reflected in a drop of the load-time curve, and sudden decrease of AE energy. Thus, in the whole loading process, AE energy clearly reflected the loading deformation and failure process of the coal samples.

Accordingly, the accumulated AE energy with time could also characterize the loading and deformation failure process of the samples. The accumulated AE energy remained at the low level at the initial stage of loading, which indicated cracks compaction only radiated a little AE energy. Interestingly, the slope of the accumulated AE energy curve increased steadily, which was induced by the expansion of the original microcracks and formation of new cracks. With cracks linking to form the fractures net and macro failure, the accumulated AE energy curve of individual sample increased sharply. The accumulated AE energy curve tended to be in stationary phase after coal failure, during which cracks evolution restored to be calm.

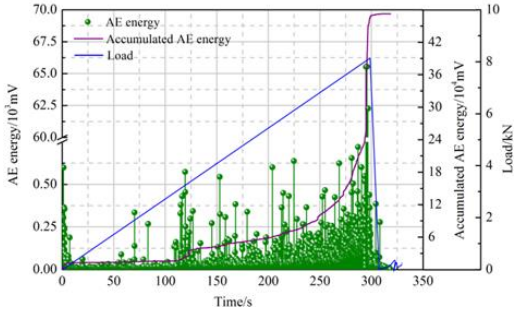

(a)

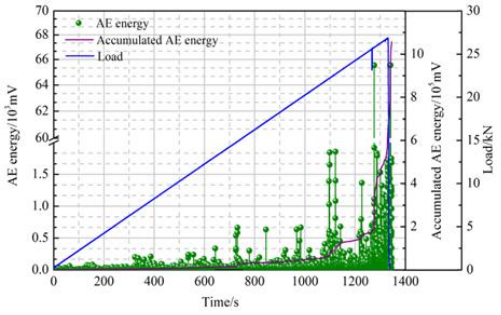

(b)

Fig. 6 Acoustic emission energy responses in the loading process. (a) sample 2, (b) sample 5, (c) sample 7, (d) sample 8, (e) sample 10, (f) sample 11, (g) sample 13 and (h) sample 16

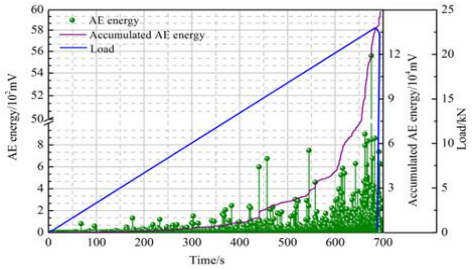

(c)

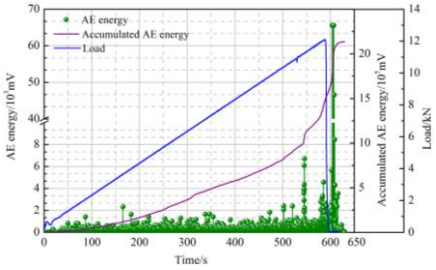

(d)

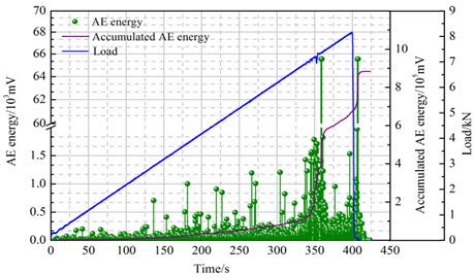

(e)

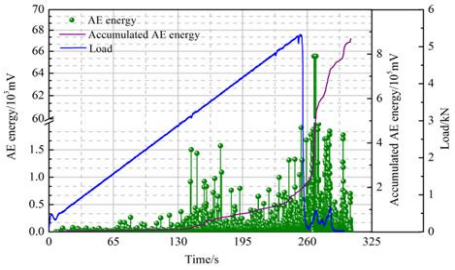

(f)

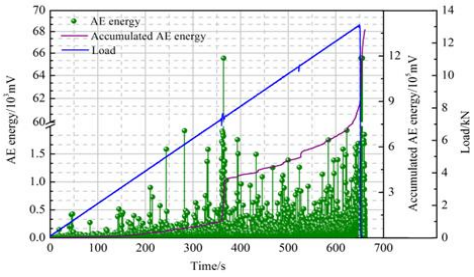

(g)

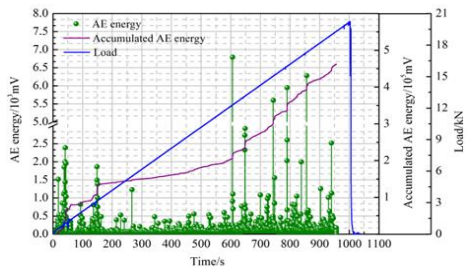

(h)

Fig. 6 Continued

4.2 Multifractal of AE energy

AE signals reflected cracks evolution and failure process of coal samples. In order to explore AE causes, the multifractal characteristics of AE would be researched.

Multifractal spectrum of AE energy time series were calculated using the box dimension method. The collected AE energy $\{x_i\}$ was divided into N subsets of length ε, and the probability distribution of each subset $\{P_i(\varepsilon)\}$ was calculated. If the time series met the multifractal characteristics, then the probability distribution function $\{P_i(\varepsilon)\}$ satisfied the following equation (partition scale $\varepsilon \to 0$)

$$\{P_i(\varepsilon)\} \propto \varepsilon^{\alpha} \tag{1}$$

where α is a constant, called singularity index, which controls the singularity of $\{P_i(\varepsilon)\}$. his reflects the properties of probability distribution with ε, which is the degree of uneven distribution of probability subsets.

If the subset marked by α had the number of units with the same probability, then it was denoted as $N_\alpha(\varepsilon)$ (see Eq. (2)). In general, the smaller the partition scale ε, the more the number of subsets obtained. Thus, $N_\alpha(\varepsilon)$ decreased with ε

$$N_\alpha(\varepsilon) \propto \varepsilon^{-f(\alpha)} \tag{2}$$

where $f(\alpha)$ is the frequency of the represented subset accounting for the whole set, that is, the fractal dimension of the α subset.

Based on these definitions, however, it was difficult to calculate the multifractal dimension. The multifractal spectrum analysis was performed using a statistical physics method (Miranda and Sharma 2016, Hu *et al.* 2014). First, a partition function was defined as follows

$$X_q(\varepsilon) \equiv \sum P_i(\varepsilon)^q \sim \varepsilon^{\tau(q)} \tag{3}$$

where $X_q(\varepsilon)$ is the defined distribution function, also known as statistical moment. $\tau(q)$ denotes the quality index with $-\infty<q<+\infty$; when $|q|$ reaches a certain value, the calculation of the multifractal spectrum region becomes stable. Therefore, q can be restricted to a certain range in the calculation.

By applying logarithm on both sides of Eq. (3), the following equation was obtained

$$\ln X_q(\varepsilon) \sim \tau(q) \ln \varepsilon \tag{4}$$

Therefore, the slope $\tau(q)$ about the double logarithmic curve of $\ln X_q(\varepsilon)$-$\ln \varepsilon$ satisfied the strict linear relationship, that was

$$\tau(q) = \lim_{\varepsilon \to 0} \frac{\ln X_q(\varepsilon)}{\ln \varepsilon} \tag{5}$$

Applying the Legendre transform of $\tau(q)$-q, the following equations were obtained

$$\alpha = \frac{d(\tau(q))}{dq} = \frac{d}{dq}\left(\lim_{\varepsilon \to 0} \frac{\ln X_q(\varepsilon)}{\ln \varepsilon}\right) \tag{6}$$

$$f(\alpha) = \alpha q - \tau(q) \tag{7}$$

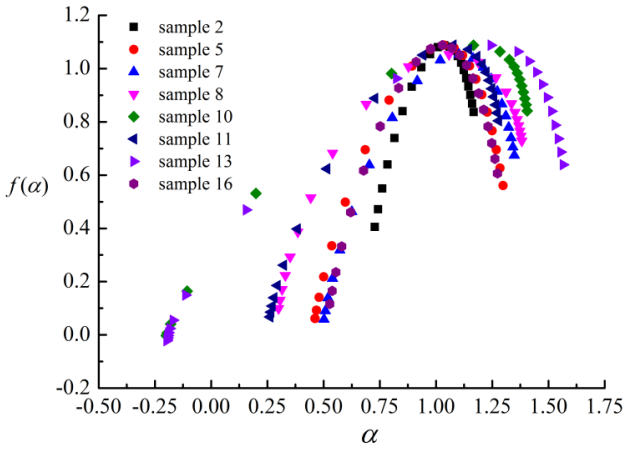

Fig. 7 Multifractal spectra $f(a) - a$ of AE energy

The curve α–$f(\alpha)$, which was composed of α and $f(\alpha)$, was the multifractal spectrum of the calculated sequence. This could reflect the nature of the nonuniform distribution of the time series $\{x_i\}$.

Based on the above equations, the program was designed to handle AE energy time sequences data by Matlab 2010b. Then the multifractal spectra of various samples were obtained, which showed in Fig. 7.

Let α represent a subset of AE energy signals; one of its subsets, represented by α_{min}, corresponds to the largest signal in the AE energy sequences, and another subset, represented by α_{max}, corresponds to the smallest signal in AE energy sequences. From Fig. 7, it could be seen that the multifractal spectrum was not symmetrical, and it was more concentrated in the right side, illustrating that the frequency of small signals was much more than that of large signals in AE energy sequences. During coal sample loading, the microdamage events and small rupture events dominated. However, the major macrofracture events usually occurred at the time of sample failure. Multifractal spectrum width, $\Delta\alpha=\alpha_{max}-\alpha_{min}$, can reflect the differences between the large and small AE energy signals. The greater the $\Delta\alpha$, indicating that there were greater differences between AE energy signals, the more intense AE changes. For example, $\Delta\alpha$ of sample 13 was the largest, which indicated AE energy signals differences were most obvious during the whole loading process. In contrast, AE energy signals differences of sample 2 were the smallest. In Eq. (7), $f(\alpha)$ represents the frequency of AE energy signals whose singularity is α in the whole loading process. The equation $\Delta f=f(\alpha_{max})-f(\alpha_{min})$ reflects the relationship between the frequency of the least and greatest signals in the AE energy time series. The difference of Δf about sample 10 was the greatest, suggesting that the occurrence probability of the least AE energy signals was larger than the greatest AE energy signals. Thus, the multifractal spectrum could explain AE signal frequency response. Besides, it could also describe the causes of AE events with load.

5. Conclusions

• At the initial loading stage, coal sample deformed elastically and was in capacity-bearing state. So there were no obvious changes of the macroscopic cracks on the

sample surface. As the load increased forward, the cracks expanded gradually along the trace of the original cracks, accompanied by the formation of secondary cracks. During a short period, most cracks joined together and produced a macroscopic fracture, which eventually leaded to the failure of the specimen. But the final failure modes of specimens were all shear failure, whether they were with the oblique joints, the cross cracks or without obvious joints.

• During the loading process, AE energy and accumulated AE energy corresponded well with the load curve, which could reflect the deformation and failure process of the samples. At the early stage, micro damage and small scale fracture events only induced a few AE events with less energy. At the failure point, large scale fracture leaded to a number of AE events with more energy. The multifractal spectrum could explain AE energy signals frequency responses and the causes of AE events with load. Multifractal spectrum width ($\Delta\alpha$), could reflect the differences between the large and small AE energy signals. And Δf could reflect the relationship between the frequency of the least and greatest signals in the AE energy time series.

Acknowledgments

The authors are grateful to the Fundamental Research Funds for the Central Universities (2017 BSCXB12) and the the Postgraduate Research & Practice Innovation Program of Jiangsu Province (KYCX17_1542).

References

Al-Jumaili, S.K., Holford, K.M., Eaton, M.J. and Pullin, R. (2015), "Parameter correction technique (PCT): A novel method for acoustic emission characterization in large-scale composites", *Compos. Part B Eng.*, **75**, 336-344.

Cao, S., Liu, Y. and Zhang, L. (2007), "Study on characteristics of acoustic emission in outburst coal", *Chin. J. Rock Mech. Eng.*, **26**(2), 2794-2799.

Chen, P., Wang, E.Y., Ou, J.C., Li, Z.H., Wei, M.Y. and Li, X.L. (2013), "Fractal characteristics of surface crack evolution in the process of gas-containing coal extrusion", *J. Min. Sci. Technol.*, **23**(1), 121-126.

Chen, X., Lu, W. and Sun, J. (2014), "Damage evolution of jointed rock masses under uniaxial compression based digital image analysis", *Chin. J. Rock Mech. Eng.*, **33**(6), 1149-1157.

Elaqra, H., Godin, N., Peix, G., R'Mili, M. and Fantozzi, G. (2007), "Damage evolution analysis in mortar, during compressive loading using acoustic emission and X-ray tomography: Effects of the sand/cement ratio", *Cement Concrete Res.*, **37**(5), 703-713.

Fang, J.Y., Dang, F.N. and Ding, W.H. (2015), "Fractal research on failure process of concrete under dynamic uniaxial compression based on CT scan graphics", *Earthq. Eng. Eng. Dyn.*, **35**(2), 208-214.

Feng, J.J., Wang, E.Y., Shen, R.X., Chen, L., Li, X.L. and Xu, Z.Y. (2016), "Investigation on energy dissipation and its mechanism of coal under dynamic loads", *Geomech. Eng.*, **11**(5), 657-670.

Ganne, P., Vervoorrta, A. and Wevers, M. (2007), "Quantification of pre-peak brittle damage: Correlation between acoustic emission and observed micri-fracturing", *J. Rock Mech. Rock Sci.*, **44**(5), 720-729.

Gao, B.B., Li, H.G., Li, L., Wang, X.L. and Yu, S.J. (2014), "Study of acoustic emission and fractal characteristics of soft and hard coal samples with same group", *Chin. J. Rock Mech. Eng.*, **33**, 3498-3504.

Gao, B.B., Li, H.G., Yu, S.J. and Li, L. (2013), "Acoustic emission and fractal characteristics of coal rock samples under triaxial compression", *Mech. Eng.*, **35**(6), 49-54.

He. J., Pan, J.N and Wang, A.H. (2014), "Acoustic emission characteristics of coal specimen under triaxial cyclic loading and unloading", *J. China Coal Soc.*, **39**(1), 84-90.

Hu, S.B., Wang E.Y., Li, Z.H., Shen, R.X. and Liu, J. (2014), "Time-varying multifractal characteristics and formation mechanism of loaded coal electromagnetic radiation", *Rock Mech. Rock Eng.*, **47**(5), 1821-1838.

John, S.L., Denis, T.K. and Surendra, P.S. (2001), "Measuring three-dimensional damage in concrete under compression", *ACI Mater. J.*, **98**(6), 465-475.

Kong, X.G., Wang, E.Y., Hu, S.B., Li, Z.H., Liu, X.F., Fang, B.F. and Zhan, T.Q. (2015), "Critical slowing down of acoustic emission characteristics of coal containing methane", *J. Nat. Gas Sci. Eng.*, **24**, 156-165.

Kong, X.G., Wang, E.Y., Hu, S.B., Liu, X.F., Xu, Z.Y. and Zhan, T.Q. (2017), "Research on precursory characteristics of critical slowing down before the failure of coal samples containing methane", *J. China U. Min. Technol.*, **46**(1), 1-7.

Kong, X.G., Wang, E.Y., Hu, S.B., Shen, R.X., Li, X.L. and Zhan, T.Q. (2016), "Fractal characteristics and acoustic emission of coal containing methane in triaxial compression failure", *J. Appl. Geophys.*, **124**, 139-147.

Landis, E.N., Nagyen, N. and Keane, D.T. (2003), "Microstructure and fracture in three dimensions", *Eng. Fract. Mech.*, **70**(7), 911-925.

Li, D.J., Zhao, F. and Zheng, M.J. (2014), "Fractal characteristics of cracks and fragments generated in unloading rock burst tests", *J. Min. Sci. Technol.*, **24**(6), 819-823.

Li, T., Mu, Z.L., Liu, G.J., Du, J.L. and Lu, H. (2016), "Stress spatial evolution law rockburst danger induced by coal mining in fault zone", *J. Min. Sci. Technol.*, **26**(3), 409-415.

Li, X.L., Li, Z.H., Wang, E.Y., Feng, J.J., Chen, L., Li, B.L. and Li, N. (2016a), "Analysis of natural mineral earthquake and blast based on Hilbert-Huang transform (HHT)", *J. Appl. Geophys.*, **128**, 79-86.

Li, Y.H., Liu, J.P., Zhao, X.D. and Yang, Y.J. (2009), "Study on b-value and fractal dimension of acoustic emission during rock failure process", *Rock Soil Mech.*, **30**(9), 2559-2563.

Liang, Y.P., Li, Q.M., Gu, Y.L. and Zou, Q.L. (2017), "Mechanical and acoustic emission characteristics of rock: Effect of loading and unloading confining pressure at the postpeak stage", *J. Nat. Gas Sci. Eng.*, **44**, 54-64.

Liu, C., Xue, J.H., Yu, G.F. and Cheng, X.Y. (2016), "Fractal characterization for the mining crack evolution process of overlying strata based on microseismic monitoring technology", *J. Min. Sci. Technol.*, **26**(2), 295-299.

Majewska, Z. and Mortimer, Z. (2006), "Chaotic behavior of acoustic emission induced in hard coal by gas sorption-desorption", *Acta Geophysica*, **54**(1), 50-59.

Majewska, Z. and Ziętek, J. (2007), "Changes of acoustic emission and strain in hard coal during gas sorption-desorption cycles", *J. Coal Geol*, **70**(4), 305-312.

Miranda F.G. and Sharma, S.R. (2016), "Multifractal analysis of lightning channel for different categories of lightning", *J. Atmos. Sol-Terr. Phys.*, **145**, 34-44.

Shkuratnik, V.L., Filimonov, Y.L. and Kuchurin, S.V. (2004), "Experimental investigations into acoustic emission in coal samples under uniaxial loading", *J. Min. Sci.*, **40**(5), 458−464.

Shkuratnik, V.L., Filimonov, Y.L. and Kuchurin, S.V. (2005),

"Experimental regularities of acoustic emission in coal samples under triaxial compression", *J. Min. Sci*., **41**(1), 44−53.

Song, D.Z., Wang, E.Y., Li, Z.H., Qiu, L.M. and Xu, Z.Y., (2017), "EMR: An effective method for monitoring and warning of rock burst hazard", *Geomech. Eng*., **12**(1), 53-69.

Tian, W., Dang, F.N. and Chen, H.Q. (2012) "Fractal Analysis on Meso-fracture of Concrete Based on the Technique of CT Image Processing", *J. Basic Sci. Eng*., **20**(30), 424-431.

Wang, E.Y., He, X.Q., Liu, X.F., Li, Z.H., Wang, C. and Xiao, D. (2011), "A non-contact mine pressure evaluation method by electromagnetic radiation", *J. Appl. Geophys*., **75**(2), 338-344.

Wang, J.A. and Li, F. (2015), "Review of inverse optimal algorithm of in-situ stress field and new achievement", *J. China U. Min. Technol*., **44**(203), 189-205.

Yan, F.Z., Lin, B.Q., Zhu, C.J., Shen, C.M., Zou, Q.L., Guo, C. and Liu, T. (2015), "A novel ECBM extraction technology based on the integration of hydraulic slotting and hydraulic fracturing", *J. Nat. Gas Sci. Eng*., **22**, 571-579.

Yin, Q., Jing, H.W., Su, H.J., Zhang, K. and Zhu, T.T. (2016), "Strength characteristics and crack coalescence evolution of granite specimens containing orthogonal filling fissures under uniaxial compression", *J. China U. Min. Technol*., **45**(209), 225-232.

Zitto, M.E., Piotrkowski, R., Gallego, A., Sagasta, F. and Benavent-Climent, A. (2015), "Damage assessed by wavelet scale band sand b-value in dynamical tests of a reinforced concrete slab monitored with acoustic emission", *Mech. Syst. Signal Pr*., **60**, 75-89.

Zou, Q.L., Lin, B.Q., Liang, J.Y., Liu, T., Zhou, Y., Yan, F.Z. and Zhu, C.J. (2014), "Variation in the pore structure of coal after hydraulic slotting and gas drainage", *Adsorpt. Sci. Technol*., **32**(8), 647-666.

JS